Eur. Phys. J. A **17**, 275–284 (2003)
DOI 10.1140/epja/i2002-10151-4

THE EUROPEAN PHYSICAL JOURNAL A

In-medium spectral functions of charmonia studied by $\bar{\mathrm{p}} + \mathrm{A}$ reactions*

Ye.S. Golubeva[1], E.L. Bratkovskaya[2], W. Cassing[3,a], and L.A. Kondratyuk[4]

[1] Institute for Nuclear Research, 60th October Anniversary Prospect 7A, 117312 Moscow, Russia
[2] Institut für Theoretische Physik, Universität Frankfurt, Robert-Mayer Str. 8-10, D-60054 Frankfurt am Main, Germany
[3] Institut für Theoretische Physik, Universität Giessen, Heinrich-Buff-Ring 16, D-35392 Giessen, Germany
[4] Institute of Theoretical and Experimental Physics, B. Cheremushkinskaya 25, 117259 Moscow, Russia

Received: 19 December 2002 /
Published online: 5 June 2003 –
Communicated by V.V. Anisovich

Abstract. We study the perspectives of resonant charmonium production in $\bar{p} + A$ reactions within the Multiple Scattering Monte Carlo (MSMC) approach. We calculate the production of the resonances $\Psi(2S)$ and $\Psi(3770)$ on various nuclei, their propagation and decay to dileptons and $D + \bar{D}$ in the medium and vacuum, respectively, employing parametrizations for the $D, \bar{D}$ self-energies taken from QCD sum rule studies. The elastic and inelastic interactions of the charmonia and open-charm mesons in the medium are taken into account, too. It is found that the $D, \bar{D}$ invariant-mass spectra from light and heavy nuclei are not sufficiently sensitive to the in-medium properties of the $\Psi(2S)$ and $\Psi(3770)$. However, a "suppression" of low-mass dileptons from the $\Psi(3770)$ might be seen experimentally as well as a small broadening of the $\Psi(2S)$ dilepton spectra.

PACS. 25.43.+t Antiproton-induced reactions – 14.40.Lb Charmed mesons – 14.65.Dw Charmed quarks – 13.25.Ft Decays of charmed mesons

1 Introduction

The dynamics of charmonia and open-charm mesons at finite baryon density and/or temperature has gained sizeable interest especially in the context of a phase transition from hadronic matter to a quark-gluon plasma (QGP), where charmed-meson states should no longer be formed due to color screening [1,2]. However, the suppression of the $c\bar{c}$ vector mesons in the high-density phase of nucleus-nucleus collisions as seen by the NA50 Collaboration [3] might also be attributed to inelastic comover scattering (cf. [4–9] and references therein) if the corresponding charmonium-hadron cross-sections are in the order of a few mb [10–15]. Theoretical models here differ in their predictions by at least an order of magnitude [16] such that at present no stringent conclusions can be drawn. As pointed out by Seth [17], this uncertainty can be substantially reduced by experimental data from $\bar{p}$-induced reactions on nuclei, where charmonia can be formed on resonance with moderate momenta relative to the target nucleus. Such studies might be performed experimentally at the HESR, which is proposed as a future facility at GSI-Darmstadt [18].

In previous studies we have explored the perspectives of charmed meson-nucleon scattering in the $\bar{p}d$ reaction [19], where the charmonium is produced on resonance with the proton in the deuteron and may scatter with the spectator neutron. We have also investigated the production of the resonances $\Psi(3770)$, $\Psi(4040)$ and $\Psi(4160)$ on various nuclei, their propagation and decay to $D, \bar{D}, D^*, \bar{D}^*, D_s, \bar{D}_s$ in the medium and vacuum [20], respectively. Furthermore, the elastic and inelastic interactions of the charmonia and open-charm mesons in the medium have been followed up in the Multiple Scattering Monte Carlo (MSMC) approach to study the collisional effects as a function of the target mass A [20]. In our previous studies we have discarded the real part of the meson self-energies $\Re\Pi(M)$; the latter can be expressed as single-particle potentials or "mass shifts" via $\Re\Pi/(2M)$ and might be calculated by dispersion relations.

Another way of getting information about mass shifts of hadrons in the medium are QCD sum rules. Related studies for J/Ψ-mesons suggest that the mass shift $\Re\Pi_V/(2M_V)$ at normal nuclear-matter density is only in the order of a few MeV [21,22] due to a small coupling of the $(c, \bar{c})$-quarks to the nuclear medium. We thus will assume $\Re\Pi_V \approx 0$ $(V = J/\Psi, \Psi(2S), \Psi(3770))$ throughout the following study. However, the open-charm mesons

* Supported by DFG, RFFI and Forschungszentrum Jülich.
[a] e-mail: Wolfgang.Cassing@theo.physik.uni-giessen.de

$(D, \bar{D}, D^*, \bar{D}^*)$ are expected to show sizeable mass shifts due to their light-quark content [23–26] in analogy to the kaons and antikaons. Especially for dropping $D, \bar{D}$ effective masses in the medium the decay width of the vector mesons then should be enhanced at finite density ρ_A as suggested in ref. [25].

We recall, that experiments on $K^{\pm}$ production from nucleus-nucleus collisions at SIS energies of 1-2 A · GeV have shown that in-medium properties of the kaons are seen in the collective flow pattern of K^+-mesons both, in-plane and out-of-plane, as well as in the abundancy and spectra of antikaons [7,27–31]. In-medium modifications of the mesons have become a topic of substantial interest in the last decade triggered in part by the early suggestion of Brown and Rho [32,33], that the modifications of hadron masses should scale with the scalar quark condensate $\langle q\bar{q}\rangle$ at finite baryon density. Thus, in view of the analogy to the $K^{\pm}$-mesons —exchanging $(s, \bar{s})$- by $(c, \bar{c})$-quarks— in-medium modifications of the open-charm mesons $D, \bar{D}$ should be observable, too. First exploratory studies by Sibirtsev *et al.* [23] have suggested also an enhanced production of $(D, \bar{D})$-mesons in $\bar{p} + A$ reactions at subthreshold energies. Such enhanced cross-sections should even more prominently be seen in central Au + Au collisions from 20 to 25 A · GeV as advocated in ref. [34]. However, some note of caution appears necessary since enhanced cross-sections might arise due to secondary reactions channels [35,36] and thus do not provide a unique signal for in-medium mass shifts. It is the aim of the present work to explore the possibility, if such mass shifts for open-charm mesons might be extracted directly from dilepton or $D, \bar{D}$ invariant-mass spectroscopy.

Our work is organized as follows: In sect. 2 we will briefly describe the input cross-sections to the MSMC approach and evaluate the formation cross-sections for the resonances $\Psi(2S)$ and $\Psi(3770)$ on protons and nuclei. The fractional decay of these resonances to open-charm mesons and dileptons in the medium and vacuum, respectively, is calculated in sect. 3 using "free" and "in-medium" spectral functions. Section 4 concludes this paper with a summary and discussion of open problems.

2 Resonance production and decay in p̄A reactions

We here examine the possibility to measure the in-medium lifetime (or total width) of the resonances $V = (\Psi(2S), \Psi(3770))$ produced in $\bar{p}A$ reactions. To this aim, we describe the vector-meson spectral function by a Breit-Wigner distribution:

$$A_V(M^2) = N_V \frac{M\Gamma^V_{\rm tot}(M)}{(M^2 - M_V^2 - \Re\Pi_V(M))^2 + M^2\Gamma^2_{\rm tot}(M)}, \quad (1)$$

where M_V denotes the vacuum pole mass, $\Re\Pi_V$ is the vector-meson self-energy in the medium —which vanishes in the vacuum— and $N_V \sim 1/\pi$ (for small width $\Gamma_{\rm tot}$) is a normalization factor that ensures $\int {\rm d}M^2 A(M^2) = 1$. The total width $\Gamma_{\rm tot}$ is separated into decay and collisional contributions as

$$\Gamma_{\rm tot}(M, \rho_A) = \Gamma_{\rm dec}(M, \rho_A) + \Gamma_{\rm coll}(M, \rho_A), \quad (2)$$

where

$$\Gamma_{\rm dec}(M, \rho_A) = \sum_c \Gamma_c(M, \rho_A) \quad (3)$$

with $\Gamma_c(M, \rho_A)$ denoting the partial width to the decay channels $c \equiv D\bar{D}, D\bar{D}^*, D^*\bar{D}$, $e^+e^-, \mu^+\mu^-$ etc., respectively. If the $(D, \bar{D})$-meson properties change with density ρ_A, this will modify the total and partial widths accordingly. The partial widths for electromagnetic decays, furthermore, are assumed to be independent of the nuclear medium.

The in-medium collisional width $\Gamma_{\rm coll}(M, \rho_A)$ in (2) is determined from the imaginary part of the forward vector-meson nucleon scattering amplitude as

$$\Gamma_{\rm coll} = \frac{4\pi}{M_V} \Im f_V(0) \rho_A, \quad (4)$$

where ρ_A again denotes the nuclear density. Furthermore, $\Im f_V(0)$ is determined via the optical theorem by the total vector-meson nucleon cross-section σ_{VN} that will be specified below.

2.1 In-medium properties of open-charm mesons

Whereas the pole masses and widths of the vector mesons M_V and open charm mesons in vacuum are rather well known [37], we have to model the in-medium properties that enter the spectral function (1) via (2) and (3). As noted before, there should be also shifts of the vector-meson pole masses by $\Re\Pi_V(M)$. According to QCD sum rule results [21] the J/Ψ meson mass shift is only in the order of a few MeV at nuclear-matter density ρ_0 and thus of minor importance. However, QCD sum rules have limited predictive power for the excited states $\Psi(2S)$ and $\Psi(3770)$ and sizeable mass shifts might occur, *e.g.*, from $D\bar{D}$ loops in case of the $\Psi(3770)$ [38]. Here, we do not speculate on such effects and will discard explicit mass shifts of the $\Psi(2S)$ and $\Psi(3770)$ and concentrate on the modification of the decay channels in the medium. To this end, in each channel c the relative decay to mesons m_1 and m_2 is described by a matrix element (squared) and phase space, *i.e.*

$$\Gamma_c \sim |\mathcal{M}_c|^2 p_c^3, \quad (5)$$

where p_c is the meson momentum in the rest frame of the resonance. The assumption (5) should hold in leading order, however, might fail if the vector meson has an explicit internal structure as advocated *e.g.* in ref. [39]. Nevertheless, in case of the $\Psi(3770)$ only the lowest channel to $D\bar{D}$ contributes such that the matrix element in (5) can be fixed by the total width at half-maximum in vacuum, which we take as $\Gamma_{\rm FWHM} = 25$ MeV [37]. We assume the same matrix element also for the $\Psi(2S)$, which

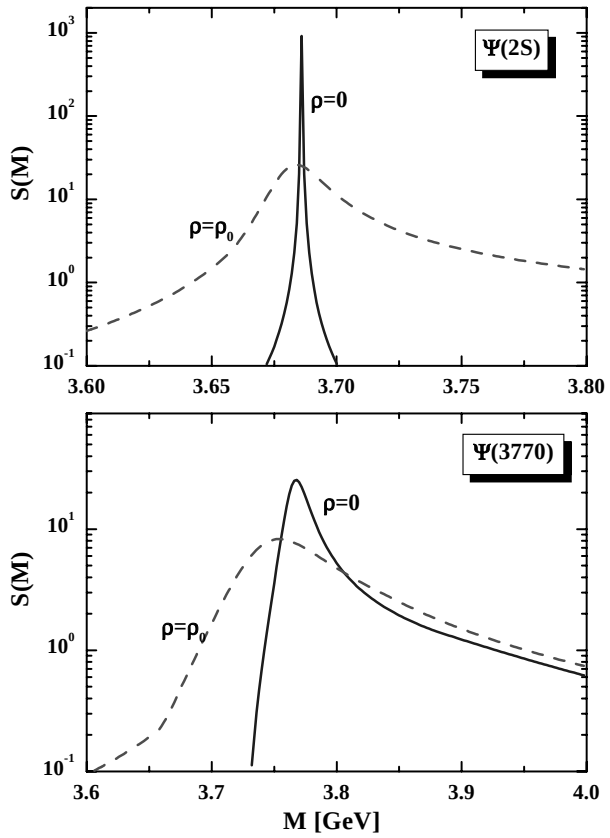

Fig. 1. The spectral functions $S(M)$ for the $\Psi(2S)$ (upper part) and $\Psi(3770)$ (lower part) in "free" space (solid lines) and at density ρ_0 (dashed lines) according to the model described in the text.

cannot be controlled experimentally since this state (of mass 3.686 GeV) is below the $D + \bar{D}$ threshold. The resulting spectral functions $S(M) = 2MA(M)$ —including the electromagnetic and light hadron decay widths— are shown in fig. 1 for the $\Psi(2S)$ (upper part) and $\Psi(3770)$ (lower part) for the "free" case by the solid lines.

In the nuclear medium the $(D, \bar{D})$-mesons are expected to show attractive mass shifts approximately linear in the density ρ_A according to the QCD sum rule studies in ref. [25]. We thus adopt

$$\Delta M_{D/\bar{D}} \approx -\alpha_{D/\bar{D}}(p)\frac{\rho_A}{\rho_0}\,, \qquad (6)$$

where p denotes the meson momentum relative to the nuclear target at rest and $\rho_0 \approx 0.168$ fm^{-3} the nuclear-matter density. The coefficients $\alpha_{D/\bar{D}}(p)$ should be determined by a microscopic theory; however, we will first approximate them by the constants $\alpha_D = 0.06$ MeV and $\alpha_{\bar{D}} = 0.01$ MeV, respectively, following the suggestions in ref. [25]. Since an explicit momentum dependence of these coefficients is expected to reduce the self-energy effects for high momenta, this particular model should lead to upper estimates for the medium effects.

With the in-medium masses for $D, \bar{D}$ fixed by (6) we can calculate the in-medium decay widths of the charm vector mesons (5) and via (4) the total decay width (2) assuming a total VN cross-section of 6 mb, which is extracted from the J/Ψ absorption data of the NA50 Collaboration [3]. Note that photoproduction of J/Ψ's on nucleons give a total J/Ψ-N cross-section of 3-4 mb [40]; however, the $\Psi(2S)$ and $\Psi(3770)$ cross-sections with nucleons should be larger by about a factor of 2, due to their larger radial size. The resulting spectral functions $S(M) = 2MA(M)$ —including again the electromagnetic and light-hadron decay widths— are shown in fig. 1 for the $\Psi(2S)$ (upper part) and $\Psi(3770)$ (lower part) for nuclear-matter density ρ_0 by the dashed lines. We observe substantially broadened spectral functions for the $\Psi(2S)$ as well as $\Psi(3770)$ due to collisional broadening (≈ 15 MeV) and a larger phase space for $D + \bar{D}$ decay. Note, that the threshold for $D + \bar{D}$ decay according to (6) at density ρ_0 moves down to 3.668 GeV —which is 18 MeV below the $\Psi(2S)$ pole mass of 3.686 GeV— such that a larger fraction of the $\Psi(2S)$ spectral distribution can decay to $D + \bar{D}$ in the medium. The lifetime of this resonance decreases accordingly from 656 fm/c in free space to ~ 9 fm/c at density ρ_0 such that some fraction of the $\Psi(2S)$ is expected to decay inside heavy nuclei such as ^{208}Pb.

2.2 Production cross-sections in p̄p and p̄A reactions

The mass differential production of the vector mesons in $\bar{p}p$ reactions can be described by Breit-Wigner resonance formation on the basis of the spectral function $A(M^2)$ (1) —employing the proper kinematics— provided that the branching of $\bar{p}p \to V$ is known,

$$\sigma_V(M) = \frac{3}{4}\,\mathrm{Br}_{p\bar{p}\to V}\; 4MA_V(M)\;\Gamma_V^{\mathrm{tot}}(M)\;\frac{\pi^2}{k^2}, \qquad (7)$$

where the factor 3/4 stems from the ratio of spin factors and k denotes the momentum of the p (or $\bar{p}$) in the cms. Following our previous works [19,20] we adopt $\mathrm{Br}(p\bar{p} \to \Psi(3770)) \approx 2 \times 10^{-4}$ which is very similar to the branching of the $\Psi(2S)$ state [37]. The resulting cross-sections for the mesons V in $\bar{p}p$ reactions are displayed in fig. 2 (upper part) as a function of the antiproton kinetic energy $T_{\bar{p}}(= T)$ in the laboratory reflecting the resonance structure (1) and the kinematics from (7) in free space. Note that, due to the small width of the $\Psi(2S)$ ($\Gamma_{\mathrm{tot}} \approx 0.3$ MeV), the kinematics have to match the resonance conditions very well.

In order to simulate events for the reaction $\bar{p}A \to V$, we use the Multiple Scattering Monte Carlo (MSMC) approach. An earlier version of this approach —denoted as Intra-Nuclear Cascade (INC) model— has been applied to the analysis of η and ω production in $\bar{p}A$ and pA interactions in refs. [41–44]. The production of the hidden-charm vector resonances on nuclei then can be evaluated within the MSMC by propagating the antiproton in the nucleus and calculating the elementary $\bar{p}p \to V$ production cross-section at the annihilation point, where the local momentum distribution is taken into account in the local Thomas-Fermi approximation.

The numerical results for the formation cross-sections of the resonances $\Psi(2S)$ and $\Psi(3770)$ on ^{208}Pb are shown

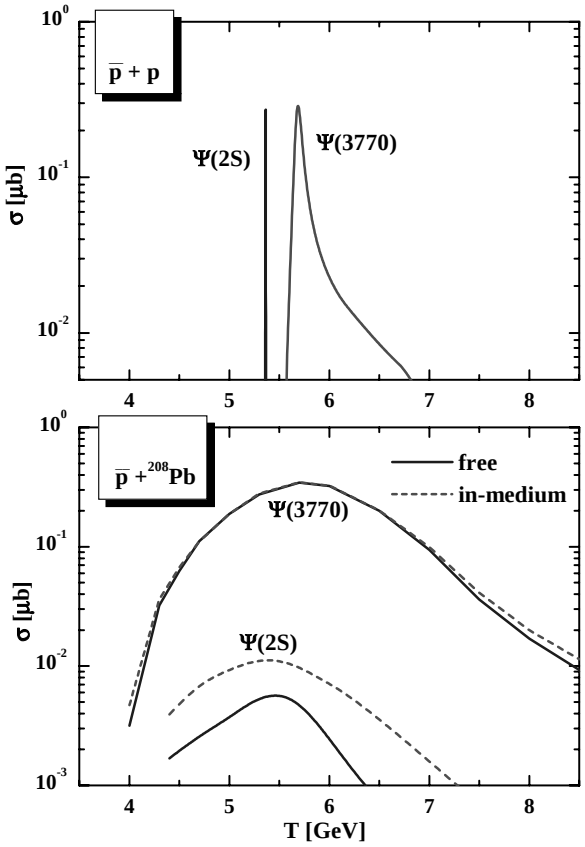

Fig. 2. The calculated cross-sections for $\Psi(2S)$ and $\Psi(3770)$ for $\bar{p}p$ (upper part) and $\bar{p} + {}^{208}$Pb reactions (lower part) as a function of the antiproton kinetic energy T in the laboratory employing "free" (solid lines) and "in-medium" spectral functions (dashed lines) as described in the text. Note, that no rescattering effects are included in these primary formation cross-sections.

in the lower part of fig. 2 as a function of $T_{\bar{p}}$ —using the "free" spectral functions (solid lines)— indicating that the resonance formation is further smeared out by the Fermi motion and the maximum in the cross-section becomes much reduced in case of the $\Psi(2S)$, in spite of the larger $\bar{p}$ annihilation cross-section on ^{208}Pb. As discussed in more detail in ref. [20], the averaging over the Fermi motion in the target leads to kinematical conditions that do not match the resonance properties in case of a small total width and thus lead to a suppression of resonance formation. For the $\Psi(3770)$ and its width of ~ 25 MeV the Fermi averaging is less crucial and compensated at $T_{\bar{p}} = 5.7$ GeV by the larger geometrical size of the Pb target.

The formation cross-section modifies only slightly for the $\Psi(3770)$ (dashed line) when employing the density-dependent in-medium spectral function as described above. Thus the excitation function in the antiproton (lab.) kinetic energy $T_{\bar{p}}$ does not provide relevant information on the medium modifications of the $\Psi(3770)$ due to the dominance of the Fermi motion in the nuclear target. The situation is different for the $\Psi(2S)$, since here a large increase in the total width is expected in the medium (cf. fig. 1). As a consequence, the relative suppression by Fermi smearing becomes less pronounced and we end up with a sizeably enhanced cross-section on nuclei for the in-medium case. Note, however, that $\Psi(2S)$-N dissociation reactions will reduce this enhancement again as well as in-medium $D + \bar{D}$ decays such that the net effect to be seen in the e^+e^- channel is even a $\sim 40\%$ reduction of the formation cross-section relative to a calculation with a "free" spectral function (see below).

2.3 Vector-meson propagation and decay

Necessary parameters for a Monte Carlo (MC) simulation of rescattering are the elastic and inelastic VN scattering cross-sections and slope parameters b for the differential elastic cross-sections $\mathrm{d}\sigma_{\mathrm{el}}/\mathrm{d}t$, which are approximated by

$$\frac{\mathrm{d}\sigma_{\mathrm{el}}}{\mathrm{d}t} \sim \exp(bt), \tag{8}$$

where t is the momentum transfer squared. These parameters as well as the masses of the rescattered particles determine the momentum and angular distributions of the particles in the final state. As in our previous studies [19, 20] we use $b = 1$ GeV^{-2} for $D, \bar{D} + N$ and VN scattering as an educated guess.

Furthermore, the inelastic cross-sections of the vector mesons with nucleons have to be specified. Since the relative momenta in the V-N system for rescattering are in the order of a few GeV, one might use high-energy geometric cross-sections for the dissociation to open-charm mesons. For the two resonances studied here we adopt an inelastic cross-section of 6 mb as well as $\sigma_{\mathrm{el}} = 1$ mb. As mentioned above, the inelastic cross-section of 6 mb is larger by about a factor of ~ 2 in comparison to the J/Ψ-N cross-section due to the larger size of the radially excited states.

The resonances are propagated with their actual mass M —selected by MC according to the in-medium spectral function (1)— with velocity p_V/E_V and decay in time according to the differential equation

$$\frac{\mathrm{d}P_V(M)}{\mathrm{d}t} = -\frac{1}{\gamma}\ \Gamma^V_{\mathrm{tot}}(M, \rho_A)\ P_V(t) \tag{9}$$

with the total width (2), while γ denotes the Lorentz γ-factor. Their decay to dileptons or $D\bar{D}$ is, furthermore, determined by Monte Carlo according to the mass differential branching ratios at the local density ρ_A. The off-shell propagation of the charmonia and evolution of their spectral functions is performed in line with the off-shell transport equations developed in refs. [45].

The open-charm mesons from the decaying vector mesons in the present case have a light-quark $q = (u, d)$ content apart from the $\bar{c}$- or c-quark. In the constituent quark model we get $D^+ = (c\bar{d})$, $D^- = (\bar{c}d)$, $\bar{D}^0 = (\bar{c}u)$, $D^0 = (c\bar{u})$ and the same composition for the related vector states. In order to estimate their elastic and inelastic cross-section with nucleons, we use the analogy to KN and $\bar{K}N$ interactions. It is well established experimentally from K^+p and K^-p reactions that light-quark exchanges with

nucleons ((uud) or (udd)) have different strength. Whereas the $K^+(u\bar{s})$ scatters only elastically with nucleons at low momentum —since the $\bar{s}$ cannot be exchanged with a light quark of a nucleon— the $K^-(s\bar{u})$ cross-section is dominated by resonant s-quark transfer leading to strange baryons such as Λ- or Σ-hyperons. Similar relations are expected to hold for the $(D, \bar{D})$-mesons [23], where especially the light-quark contribution should give much larger cross-section on nucleons than the $c\bar{c}$ vector resonances. This analogy is based on $SU(4)_{\rm flavor}$ symmetry [46–48] which, however, might be broken substantially in view of the different geometrical sizes of K- and D-mesons. At present this is an open question which has to be settled by experiment. Corresponding experiments have been proposed in ref. [20].

For our calculations we adopt the following cross-sections —taken as constants in the momentum regime of interest—:

$$\sigma^{\rm el}_{DN} = \sigma^{\rm el}_{\bar{D}N} = 10\,{\rm mb}\,;$$

$$\sigma^{\rm inel}_{\bar{D}N} \approx 0; \qquad \sigma^{\rm inel}_{DN} = 10\,{\rm mb}\,. \tag{10}$$

Here, the inelastic cross-sections of D-mesons refer to c-quark exchange reactions with nucleons. Furthermore, charge exchange reactions like $D^+n \leftrightarrow D^0p$ or $D^-p \leftrightarrow \bar{D}^0n$ are incorporated with a constant cross-section $\sigma_{\rm qexc.} = 12$ mb (cf. ref. [20]).

3 Resonance production in p̄A reactions

Within the model described in sect. 2 we now can calculate the cross-sections for the $c\bar{c}$ resonances in $\bar{p}A$ reactions for all targets of interest and obtain the information about in-medium resonance decays (for densities $\rho_A \geq 0.03$ fm^{-3}) or vacuum decays, respectively. We note that apart from the resonant production of open-charm mesons they may also be produced directly as $(c\bar{q})$ and $(\bar{c}q)$ pairs in $\bar{p}N$ annihilation. This channel strongly dominates in annihilation reactions on neutrons in the nucleus, since the charmonium production is forbidden by charge conservation at low energy above threshold. At higher invariant energies a pion might balance the charge in the $\Psi + \pi$ final channel. For our estimates we have employed the Regge-model analysis of ref. [49] for the elementary $\bar{p}N \to D, \bar{D}$ cross-section as also used by Sibirtsev *et al.* in refs. [23,24]. As already shown in ref. [20], the nonresonant production of $(D, \bar{D})$-pairs at $T_{\rm lab} = 5.7$ GeV is expected to be about the same as the resonant production via $\Psi(3770)$ excitation and decay in case of heavy nuclei.

3.1 Open-charm propagation and rescattering

The open-charm mesons, produced by resonance decay or nonresonant channels, rescatter in the nuclear medium either elastically or inelastically. Furthermore, they change their quasi-particle properties (or mass) dynamically according to (6) while propagating from the nuclear medium to the vacuum. This dynamical problem can be well addressed by the MSMC approach as well for all bombarding energies and targets.

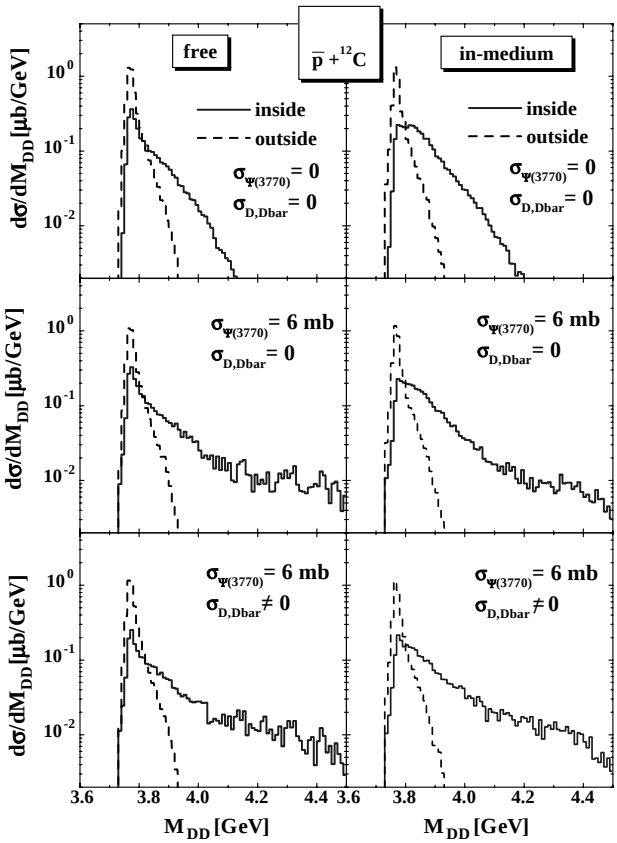

Fig. 3. The calculated $D + \bar{D}$ invariant-mass distributions for $\bar{p}+$ ^{12}C reactions at $T_{\bar{p}} = 5.7$ GeV within various limits for the "in-medium" decay (solid histograms) and "vacuum" decays (dashed histograms), respectively. The diagrams on the l.h.s. correspond to calculations with the "free" spectral function for the $\Psi(3770)$, whereas the diagrams on the r.h.s. stem from calculations with the "in-medium" spectral functions. In the upper plots the rescatterings of the $\Psi(3770)$- and $(D, \bar{D})$-mesons have been neglected, whereas in the middle plots $\Psi(3770) + N$ dissociation has been included. The lower plots additionally include the $D, \bar{D}$ elastic- and inelastic-rescattering processes as specified in sect. 2.

In order to properly interpret the final results, it is instructive to show the $D + \bar{D}$ invariant-mass spectra within different dynamical limits. To this aim we display in figs. 3 and 4 (upper left parts) the invariant-mass spectrum of $D + \bar{D}$ mesons from $\Psi(3770)$ decays in $\bar{p} +$ ^{12}C and $\bar{p} +$ ^{208}Pb reactions at $T_{\bar{p}} = 5.7$ GeV using the "free" charmonium spectral function and branching ratios while discarding open-charm and $\Psi(3770)$ rescattering. As seen from fig. 3 and fig. 4 (upper left parts), the in-medium decays to $D + \bar{D}$ (solid histograms) make up the major part of the invariant-mass distribution at masses above 3.85 GeV, since the lifetime of high-mass $\Psi(3770)$ becomes very short in nuclei. According to the same argument the lifetime of $\Psi(3770)$'s at low invariant masses is rather high due to the very limited phase space for $D + \bar{D}$ decay,

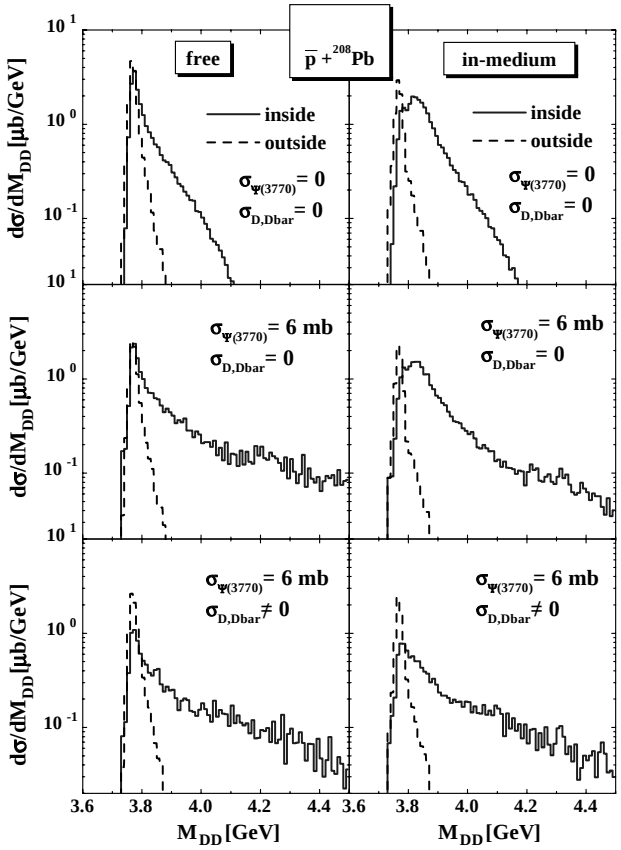

Fig. 4. The calculated $D + \bar{D}$ invariant-mass distributions for $\bar{p} +$ ^{208}Pb reactions at $T_{\bar{p}} = 5.7$ GeV within various limits for the "in-medium" decay (solid histograms) and "vacuum" decays (dashed histograms), respectively. The various calculations correspond to the same limits as in fig. 3.

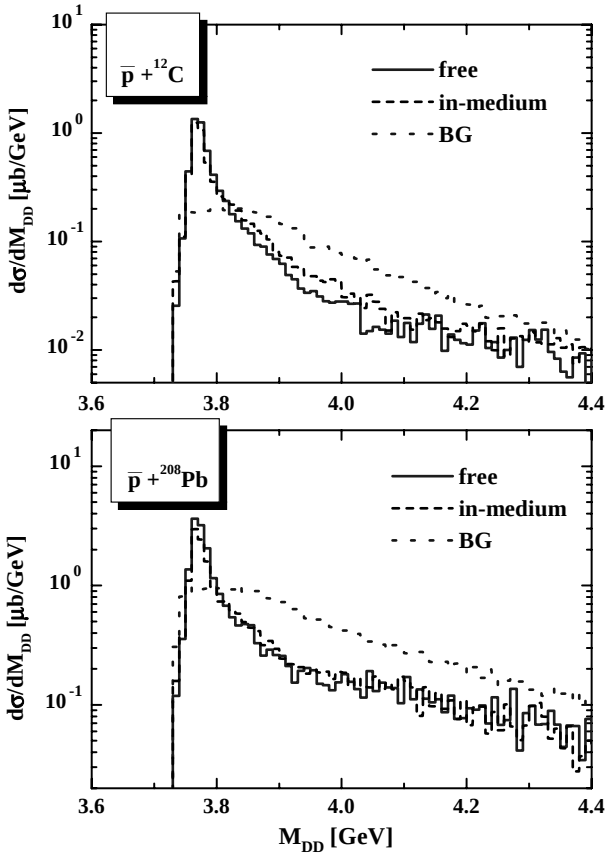

Fig. 5. The calculated $D + \bar{D}$ invariant-mass distributions for $\bar{p} +$ ^{12}C and $\bar{p} +$ ^{208}Pb reactions at $T_{\bar{p}} = 5.7$ GeV as obtained from summing up the "inside" and "outside" decay contributions from figs. 3 and 4, where all final-state interactions have been included. The solid histograms correspond to the case of the "free" $\Psi(3770)$ spectral function, while the results for the "in-medium" spectral functions are shown in terms of the dashed histograms. The dotted lines (BG) show additionally the expected background from nonresonant $D, \bar{D}$ production as calculated by 2-body final-state kinematics.

such that we obtain a preferential decay in the vacuum ($\rho_A \leq 0.03$ fm^{-3}) for invariant masses below 3.8 GeV, especially in case of the light ^{12}C target.

For the next calculations we switch on the $\Psi(3770)$-N rescattering, however, discard $D, \bar{D}$ mass shifts and rescattering (middle left parts in figs. 3 and 4). The effects of $\Psi(3770)$ rescatterings are esssentially a broadening of the $D+\bar{D}$ invariant-mass distribution to high invariant masses and a reduction of the vacuum contribution (dashed histograms) due to dissociation reactions. This rather obvious medium modification is enhanced when including $D, \bar{D}$ rescattering (lower left parts in figs. 3 and 4) which additionally leads to a depletion of the invariant-mass distribution in the resonance peak since rescattering changes the invariant mass of the $(D, \bar{D})$-pair observed asymptotically. These quite drastic medium modifications compete with the spectral changes of the $\Psi(3770)$ in the medium due to the $D, \bar{D}$ potentials.

In the r.h.s. of figs. 3 and 4 we show the corresponding $D + \bar{D}$ invariant-mass distributions for the dynamical $\Psi(3770)$ spectral function without rescatterings (upper right parts), with $\Psi(3770)$ rescattering (middle right parts) and also including $D, \bar{D}$ interactions with nucleons (lower right parts). Whereas the high-mass spectra differ substantially compared to the "free" $\Psi(3770)$ spectral function (l.h.s.) when discarding final-state interactions, the final mass spectra —including $\Psi(3770)$-N and $D, \bar{D}$ interactions— look very similar. One might have expected an enhancement in the low-mass region below 3.77 GeV, however, the in-medium decays to $D + \bar{D}$ at lower invariant masses finally show up in the vacuum at higher invariant masses (above the $D + \bar{D}$ vacuum threshold) since the open-charm mesons regain their "free" masses when moving out of the medium.

A direct comparison of the $D + \bar{D}$ invariant-mass distributions —summing up the "inside" and "outside" components— is displayed in fig. 5 for ^{12}C and ^{208}Pb for the case of the "free" spectral function (solid histograms) and the in-medium spectral functions (dashed histograms). Here, all final-state interactions have been included in the calculations. Within statistics there is practically no difference between the spectra for the Pb target such that $D + \bar{D}$ invariant-mass spectroscopy does not

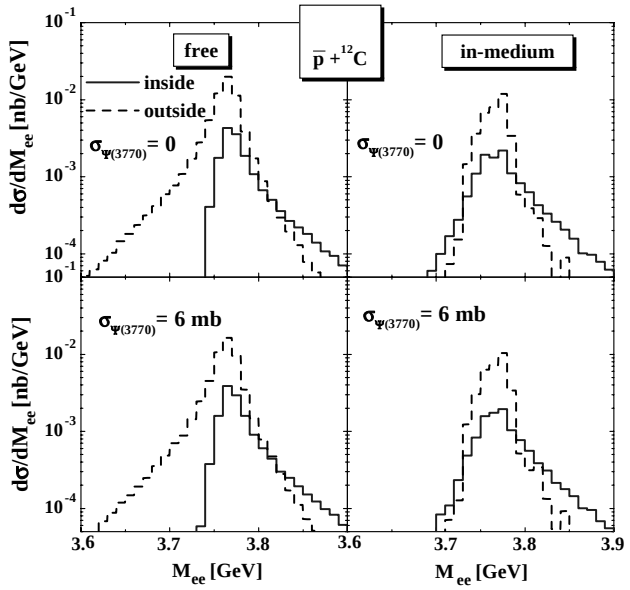

Fig. 6. The calculated e^+e^- invariant-mass distributions for $\bar{p}+$ ^{12}C reactions at $T_{\bar{p}} = 5.7$ GeV within various limits for the "in-medium" decays (solid histograms) and "vacuum" decays (dashed histograms), respectively. The diagrams on the l.h.s. correspond to calculations with the "free" spectral function for the $\Psi(3770)$, whereas the diagrams on the r.h.s. stem from calculations with the "in-medium" spectral functions. In the upper plots the rescatterings of the $\Psi(3770)$-mesons have been neglected, whereas in the lower plots $\Psi(3770) + N$ dissociation has been included.

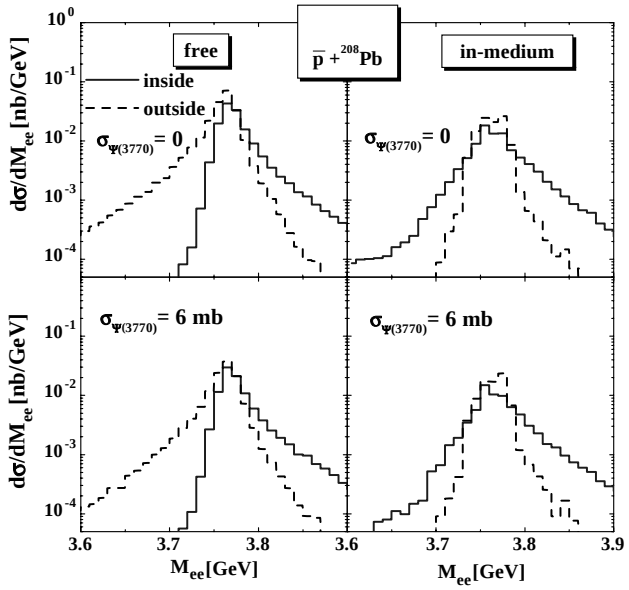

Fig. 7. The calculated e^+e^- invariant-mass distributions for $\bar{p}+$ ^{208}Pb reactions at $T_{\bar{p}} = 5.7$ GeV within various limits for the "in-medium" decay (solid histograms) and "vacuum" decays (dashed histograms), respectively. The calculations correspond to the same limits as in fig. 6 for the ^{12}C target.

qualify much to probe the in-medium $\Psi(3770)$ spectral function. This becomes even more apparent when comparing additionally to the background from nonresonant $D\bar{D}$ production (dotted lines "BG") which —integrated over invariant mass— is expected to be of comparable magnitude in cross-section at $T_{\bar{p}} = 5.7$ GeV [20]. Thus, apart from the vicinity of the resonance pole, the nonresonant background will dominate the high-mass region of the invariant-mass spectra. We mention that in order to calculate the invariant-mass distribution from the nonresonant background we have assumed 2-body S-wave kinematics for the process $\bar{p}p \to D\bar{D}$.

Without explicit representation we mention that the perspectives to study the in-medium properties of the $\Psi(2S)$ by $D + \bar{D}$ invariant-mass spectroscopy at $T_{\bar{p}} = 5.4$ GeV are rather discouraging, since the contribution from the $\Psi(3770)$ decays by far exceeds the signal from the $\Psi(2S)$ decays (cf. fig. 2) and the in-medium $D, \bar{D}$ move on-shell again, such that only a tiny contribution above threshold survives. According to the authors point of view such tiny effects will be extremely hard to identify experimentally.

However, it remains to be seen if the expected in-medium modifications of the charmonia might be detected via the dilepton decay mode since the e^+e^- (or $\mu^+\mu^-$) pairs do not suffer from strong final-state interactions and also have no threshold in the vicinity of the charmonium pole masses.

3.2 Resonant dilepton decays in $\bar{p}$A reactions

We continue with the e^+e^- decay modes of the charmonia that have a decay width of ~ 2.2 keV for the $\Psi(2S)$ and ~ 0.26 keV for the $\Psi(3770)$, respectively [37]. In spite of these low decay widths, the dilepton decay mode might provide essential information about the in-medium properties of the charmonia.

In our actual calculations we assume the dileptonic decay width to be constant as a function of the invariant mass $M_{e^+e^-}$ since, in case of the charmonia, the total width is very small compared to the pole masses. We start with $\Psi(3770)$ resonant production in $\bar{p}+$ ^{12}C and $\bar{p}+$ ^{208}Pb reactions at $T_{\bar{p}} = 5.7$ GeV and consider the same limits as for the $D + \bar{D}$ decay mode. The numerical invariant mass spectra for these reactions are shown in figs. 6 and 7, respectively.

As seen from figs. 6 and 7, the in-medium dilepton decays (40% for Pb) dominate for high-invariant-mass pairs, whereas the low-mass components —below the $D + \bar{D}$ threshold— only stem from vacuum decays (60% for Pb) in case of the "free" $\Psi(3770)$ spectral functions (l.h.s.). This phenomenon is easily attributed to the long lifetime of the $\Psi(3770)$ for low invariant mass such that it only decays in vacuum and "radiates" dileptons for a long time. When including $\Psi(3770)$-N dissociation reactions (lower parts of figs. 6 and 7) the shape and relative contribution from "inside" and "vacuum" decays does not change very much, only the magnitude of the mass differential cross-section is reduced for Pb by a factor of ~ 0.63. For the "in-medium" $\Psi(3770)$ spectral function the individual results look different (r.h.s.), since now the resonance can decay to $D\bar{D}$ in the medium at lower invariant masses, too,

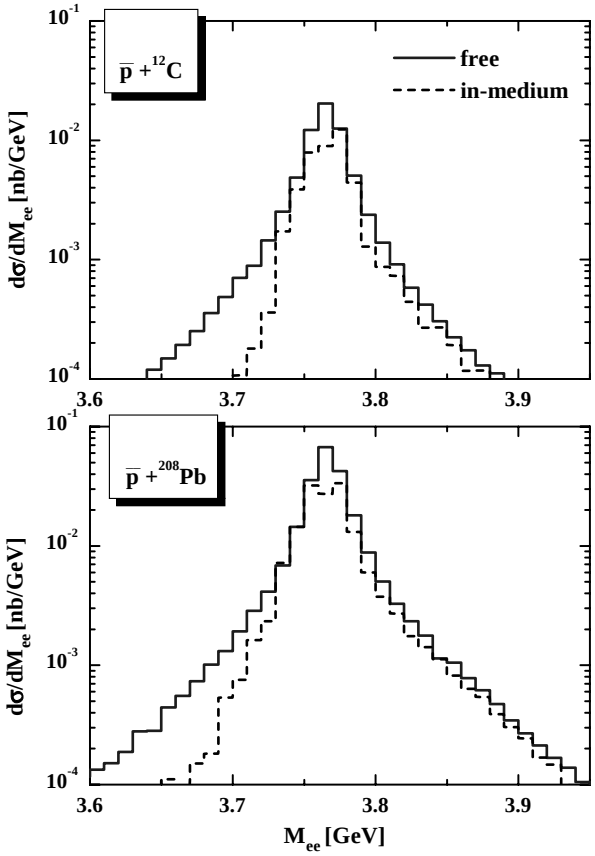

Fig. 8. The calculated e^+e^- invariant-mass distributions for $\bar{p}+$ ^{12}C and $\bar{p}+$ ^{208}Pb reactions at $T_{\bar{p}} = 5.7$ GeV as obtained from summing up the "inside" and "outside" decay contributions from figs. 6 and 7, where all final-state interactions have been included. The solid histograms correspond to the case of the "free" $\Psi(3770)$ spectral function, while the results for the in-medium spectral functions are shown in terms of the dashed histograms.

and the lifetime for low-mass $\Psi(3770)$ decreases substantially. Accordingly, there is also a large "inside" fraction of dilepton decays for lower masses which now no longer can decay in the vacuum. The result is a narrowing of the $\Psi(3770)$ spectral function in the "outside" contribution from the lower mass side. The relative contributions from "inside" and "outside" decays do not change substantially when including again $\Psi(3770) + N$ dissociation reactions (lower parts of figs. 6 and 7). Only the magnitude of the differential cross-section becomes suppressed as in case of the "free" spectral function (l.h.s.).

The net spectra (possibly) to be seen experimentally are displayed in fig. 8 for both targets in case of the "free" (solid histograms) and "in-medium" $\Psi(3770)$ spectral functions (dashed histograms) where the "inside" and "outside" components have been added up. Apart from the fact, that the differential cross-sections are below 0.02 and 0.1 nb/GeV, respectively, the medium modifications only show up in a suppression of the low-mass distributions, since the high-mass tails are practically the same. Thus the net effect is not an "enhancement" of lower-mass

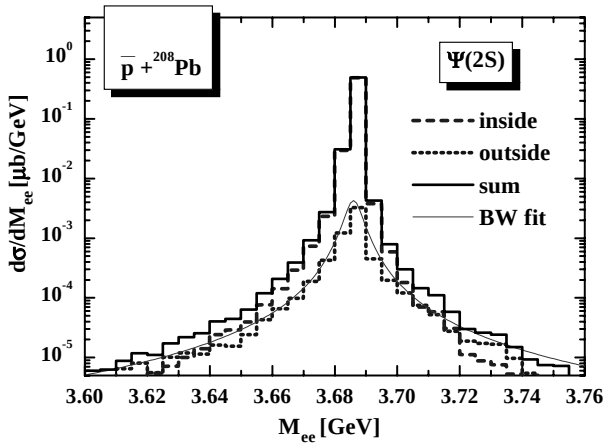

Fig. 9. The calculated e^+e^- invariant-mass distribution for $\bar{p}+$ ^{208}Pb reactions at $T_{\bar{p}} = 5.5$ GeV from the "inside" (dashed histogram) and "outside" decay contribution (dotted histogram) employing the in-medium $\Psi(2S)$ spectral function described in the text. The "inside" component can be fitted by a Breit-Wigner distribution with a width of 6 MeV (thin solid line). The total spectrum is given by the solid histogram.

dileptons as in case of the ρ- and ω-mesons [7,50], but a relative "suppression". If this suppression could be seen in experiment, it should provide valuable information on the $D, \bar{D}$ properties in the nuclear medium.

The question remains, to which extent a substantial broadening of the $\Psi(2S)$ in the medium will leave its traces in the dilepton invariant-mass spectra. Our actual calculations for the system $\bar{p}+$ ^{12}C at $T_{\bar{p}} = 5.5$ GeV show no effects within statistics since the average density in ^{12}C is substantially below nuclear-matter density and the lifetime of the $\Psi(2S)$ is large (in fm/c) compared to the size of this nucleus (in fm). For $\bar{p}+$ ^{208}Pb at $T_{\bar{p}} = 5.5$ GeV there is a small fraction of $\Psi(2S)$ (about 2%) that decays to e^+e^- inside the nucleus (dashed histogram in fig. 9) and shows a spectral distribution that is compatible with a Breit-Wigner shape of 6 MeV width (cf. thin solid line in fig. 9), which is larger by a factor of 20 than the "free" width of 0.3 MeV. However, when summing up the "inside" and "outside" dilepton decays again only a small broadening in the tails of the invariant-mass spectra survives (solid histogram in fig. 9). We note, that this effect might be hidden in the background from Drell-Yan dileptons and hard to be seen experimentally.

4 Summary

In this study we have explored the perspectives of measuring the dynamics of hidden-charm vector mesons and open-charm mesons in antiproton-induced reactions on nuclei by $D + \bar{D}$ and e^+e^- invariant-mass spectroscopy. Such experimental studies will be possible at the high-energy antiproton storage ring (HESR) proposed for the future GSI facility [18]. The Multiple Scattering Monte Carlo (MSMC) calculations have been based on the resonance production concept with resonance properties

from the PDG [37] in vacuum, however, modified in the nuclear medium according to phase space (cf. sect. 2) involving dropping masses for the D- and $\bar{D}$-mesons (6). The actual values have been taken from the QCD sum rule studies of ref. [25].

We find that for a heavy nucleus like ^{208}Pb the fraction of "inside" decays to dileptons or $D + \bar{D}$ reaches $\sim 40\%$ for the $\Psi(3770)$, which at first sight looks promising. However, the in-medium effects in the $D + \bar{D}$ invariant-mass spectra are hard to see experimentally since for invariant masses from the $D + \bar{D}$ threshold to the $\Psi(3770)$ pole mass the final spectrum is only slightly modified, while at high invariant masses it is covered by the nonresonant background (fig. 5). The e^+e^- invariant-mass spectra from the in-medium $\Psi(3770)$ show a decrease at small masses (below the $D+\bar{D}$ threshold) since these charmonia preferentially now decay via the $D + \bar{D}$ channel in the nucleus. Thus the net effect is not an "enhancement" of lower mass dileptons as in case of the ρ- and ω-mesons [7,50], but a relative "suppression". If this suppression could be seen in experiment it might provide valuable information on the $D, \bar{D}$ properties in the nuclear medium.

Furthermore, we find that for the in-medium effects incorporated the $D, \bar{D}$ decays of the $\Psi(2S)$ in the nucleus —that become possible due to a dropping of the $D, \bar{D}$ masses— are unlikely to be seen due to the much larger yield from the $\Psi(3770)$ at the same bombarding energy (fig. 2). On the other hand, a small net broadening of the $\Psi(2S)$-resonance tails survives in the dilepton channel according to our calculations (fig. 9) which, however, will be hard to separate from the Drell-Yan background.

We close in noting that the in-medium effects explored in this work are based on QCD sum rule studies for hidden-charm and open-charm mesons at vanishing relative momentum and low nuclear densities [21,25]. In the $\bar{p}+A$ reactions investigated the mesons actually have momenta of 2-4 GeV/c [20] with respect to the target at rest, such that the in-medium effects explored more likely correspond to an educated guess. If the $D, \bar{D}$ potentials (6) decrease substantially in magnitude with momentum, then all effects pointed out here will decrease accordingly and practically no medium modifications should be seen experimentally. On the other hand, the open-charm potentials (6) might be even larger in nature and thus the effects become enhanced. Nevertheless, an answer here has to come from related experimental studies, *e.g.*, at the HESR [18] which appear sufficiently promising.

This work was supported by DFG under grants No. 436 RUS 113/600, CA 124/4 and RFFI.

References

1. T. Matsui, H. Satz, Phys. Lett. B **178**, 416 (1986).
2. H. Satz, Rep. Prog. Phys. **63**, 1511 (2000).
3. NA50 Collaboration (M.C. Abreu *et al.*), Phys. Lett. B **410**, 337 (1997); **450**, 456 (1999); **477**, 28 (2000); **521**, 195 (2001).
4. N. Armesto, A. Capella, Phys. Lett. B **430**, 23 (1998).
5. A. Capella, E.G. Ferreiro, A.B. Kaidalov, Phys. Rev. Lett. **85**, 2080 (2000).
6. W. Cassing, E.L. Bratkovskaya, Nucl. Phys. A **623**, 570 (1997).
7. W. Cassing, E.L. Bratkovskaya, Phys. Rep. **308**, 65 (1999).
8. R. Vogt, Phys. Rep. **310**, 197 (1999).
9. C. Gerschel, J. Hüfner, Annu. Rev. Nucl. Part. Sci. **49**, 255 (1999).
10. K. Haglin, Phys. Rev. C **61**, 031902 (2000); K.L. Haglin, C. Gale, Phys. Rev. C **63**, 065201 (2001).
11. Y. Oh, T. Song, S.H. Lee, Phys. Rev. C **63**, 034901 (2001).
12. V.V. Ivanov, Y.L. Kalinovsky, D. Blaschke, G.R. Burau, hep-ph/0112354.
13. K. Martins, D. Blaschke, E. Quack, Phys. Rev. C **51**, 2723 (1995).
14. C.Y. Wong, E.S. Swanson, T. Barnes, Phys. Rev. C **62**, 045201 (2000); **65**, 014903 (2002).
15. W. Liu, C.M. Ko, Z.W. Lin, Phys. Rev. C **65**, 015203 (2002).
16. B. Müller, Nucl. Phys. A **661**, 272c (1999).
17. K. Seth, in *Proceedings of the International Workshop XXIX, Structure of Hadrons, on Gross Properties of Nuclei and Nuclear Excitations, Hirschegg, Austria, January 14-20, 2001*, edited by H. Feldmeier *et al.* (GSI, Darmstadt, 2001).
18. *An International Accelerator Facility for Beams of Ions and Antiprotons*, `http://www.gsi.de/GSI-Future/cdr/`.
19. W. Cassing, Ye. Golubeva, L.A. Kondratyuk, Eur. Phys. J. A **7**, 279 (2000).
20. Ye. Golubeva, W. Cassing, L.A. Kondratyuk, Eur. Phys. J. A **14**, 255 (2002).
21. F. Klingl, S. Kirn, S.H. Lee, P. Morath, W. Weise, Phys. Rev. Lett. **82**, 3396 (1999).
22. A. Hayashigaki, Prog. Theor. Phys. **101**, 923 (1999).
23. A. Sibirtsev, K. Tsushima, A.W. Thomas, Eur. Phys. J. A **6**, 351 (1999).
24. A. Sibirtsev, Nucl. Phys. A **680**, 274c (2001).
25. A. Hayashigaki, Phys. Lett. B **487**, 96 (2000).
26. K. Tsushima, D.H. Lu, A.W. Thomas, K. Saito, R.H. Landau, Phys. Rev. C **59**, 2824 (1999).
27. F. Laue *et al.*, Eur. Phys. J. A **9**, 397 (2000).
28. P. Crochet *et al.*, Phys. Lett. B **486**, 6 (2000).
29. A. Devismes for the FOPI Collaboration, J. Phys. G **28**, 1591 (2002).
30. C.M. Ko, J. Phys. G **27**, 327 (2001).
31. S. Pal, C.M. Ko, Z.-W. Lin, Phys. Rev. C **64**, 042201 (2001).
32. G.E. Brown, M. Rho, Phys. Rev. Lett. **66**, 2720 (1991).
33. G.E. Brown, M. Rho, Phys. Rep. **363**, 85 (2002).
34. W. Cassing, E.L. Bratkovskaya, A. Sibirtsev, Nucl. Phys. A **691**, 753 (2001).
35. W. Cassing, E.L. Bratkovskaya, U. Mosel, S. Teis, A. Sibirtsev, Nucl. Phys. A **614**, 415 (1997).
36. C. Hartnack, H. Oeschler, J. Aichelin, Phys. Rev. Lett. **90**, 102302 (2003).
37. Particle Data Group, Eur. Phys. J. C **15**, 1 (2000).
38. C.M. Ko, Su Houng Lee, nucl-th/0208003, to be published in Phys. Rev. C.
39. B. Friman, S.H. Lee, T. Song, Phys. Lett. B **548**, 153 (2002).
40. J. Hüfner, B.Z. Kopeliovich, Phys. Lett. B **426**, 154 (1998); Y.B. He, J. Hüfner, B.Z. Kopeliovich, Phys. Lett. B **477**, 93 (2000).

41. Ye.S. Golubeva, A.S. Iljinov, B. Krippa, I.A. Pshenichnov, Nucl.Phys. A **537**, 393 (1992).
42. Ye.S. Golubeva, A.S. Iljinov, I.A. Pshenichnov, Nucl. Phys. A **562**, 389 (1993).
43. W. Cassing, Ye.S. Golubeva, A.S. Iljinov, L.A. Kondratyuk, Phys. Lett. B **396**, 26 (1997).
44. Ye.S. Golubeva, L.A. Kondratyuk, W. Cassing, Nucl. Phys. A **625**, 832 (1997).
45. W. Cassing, S. Juchem, Nucl. Phys. A **665**, 377 (2000); **672**, 417 (2000); **677**, 445 (2000).
46. Z. Lin, C.M. Ko, Phys. Rev. C **62**, 034903 (2000); J. Phys. G **27**, 617 (2001).
47. Z. Lin, C.M. Ko, B. Zhang, Phys. Rev. C **61**, 024904 (2000).
48. B. Zhang, C.M. Ko, B.A. Li, Z.W. Lin, S. Pal, Phys. Rev. C **65**, 054909 (2002).
49. A.B. Kaidalov, P.E. Volkovitsky, Z. Phys. C **63**, 517 (1994).
50. R. Rapp, J. Wambach, Adv. Nucl. Phys. **25**, 1 (2000).